Synthesis of Hydrothermally Stable and Long-Range Ordered Ce-MCM-48 and Fe-MCM-48 Materials

Yaofeng Shao,[†] Lingzhi Wang,[†] Jinlong Zhang,*[,†] and Masakazu Anpo[‡]

Lab for Advanced Materials and Institute of Fine Chemicals, East China University of Science and Technology, 130 Meilong Road, Shanghai 200237, People's Republic of China, and Graduate School of Engineering, Osaka Prefecture University, 1-1 Gakuen-cho, Sakai, Osaka 599-8531, Japan

Received: July 21, 2005; In Final Form: September 13, 2005

The hydrothermally stable and long-range ordered Ce-MCM-48 and Fe-MCM-48 were conveniently synthesized at 393 K for 24 h by directly adding fluoride ions to the initial gel without posttreatment and pH adjustment. The Ce-MCM-48 with a Si/Ce of 200 and 100, which were prepared by directly adding fluoride ions, could still maintain their mesoporous structures after refluxing in boiling water for 3 days. The incorporation of Ce into MCM-48 could enhance the hydrothermal stability of MCM-48 in the absence of fluoride ions; however, the incorporation of Fe into MCM-48 materials barely improved the hydrothermal stability of MCM-48 materials. The effect of adding NaF was much more efficient in enhancement of hydrothermal stability than that of the incorporation of Ce. The addition of fluoride ions mainly improves the degree of polymerization of silicates. The Ce^{4+} ions in Ce-MCM-48 appear to be present partly in tetrahedral coordination in the framework and partly as CeO_2 particles on the surface of framework. The Ce positioned on the surface of pore walls and in the framework both provide the protection against water attack.

1. Introduction

Since mesoporous materials of M41S family were first reported by Mobile researchers,[1,2] increasing interest has been focused on their properties and uses.[3,4] MCM-48 has a three-dimensional channel structure, which is more attractive than MCM-41, with a one-dimensional pore system, when applied to catalytic reaction and other uses.[5] However, pure silica MCM-48 has few catalytic active sites that has limited their use in catalytic reactions; therefore, increasingly, researchers have focused on the mesoporous silica materials with substituted catalytically active heteroatoms, which have been shown to exhibit considerable reactivity due to easily accessible active sites within the mesoporous network.[6,7] The incorporation of Ce, an early member of lanthanides, in the MCM-48 silica network is expected to impart dual catalytic activity in heterogeneous acid as well as redox catalysis.[8] In addition, it is well-known that the Fe^{3+} ions are very sensitive to oxidation−reduction reactions, so incorporating Fe^{3+} ions into the framework of cubic MCM-48 may result in a good potential catalyst for oxidation reactions.[9] However, mesoporous materials generally possess low hydrothermal stability due to the amorphous nature of their frameworks[4] because the hydrothermal stability of mesoporous materials is very important with respect to their use in applications that require contact with water, especially in hot aqueous solutions, and the loss of hydrothermal stability could be a serious barrier for the application of this material. Therefore, significant effort has been directed at improving the hydrothermal stability of pure silica and heteroatom-substituted mesoporous materials.[10,11]

Generally, the hydrothermal stability of mesoporous materials can be improved by pore wall thickening,[12−15] silylation,[16−19] stabilization by salt effect,[20,21] and hydrothermal restructuring processes.[22] It is known that fluoride ions do influence the nature, activity, and polymerizing capacity of silica precursors, and a fluorinated silica surface is much more hydrophobic and more resistant to the attack of water molecules than a silanol silica surface.[23] Therefore, recently, many researches have been focused on the fluorination of MCM-48.[24,25] For instance, Kim et al.[25] reported that the hydrothermal stability of MCM-48 could be improved by posttreatment in NaF solution.

However, most present studies are focused on the improvement of the hydrothermal stability of pure silica MCM-48. Except for Al-MCM-48,[26,27] there are few reports on the heteroatom-substituted MCM-48. In consideration of the great potential applications of heteroatom-substituted MCM-48, herein, we first present a convenient method to synthesize hydrothermally stable and long-range ordered Ce-MCM-48 and Fe-MCM-48 by directly adding fluoride ions to the initial gel. Our method differs from previous reports,[24,25] and does not need any posttreatment and pH adjustment for short times. We also discuss the effect of fluoride ions in detail during the synthesis process and the effect of Ce and Fe incorporation into MCM-48 on the hydrothermal stability of mesoporous materials. In addition, this method may have the potential for preparing other heteroatom-substituted mesoporous materials with hydrothermal stability and long-range ordering.

2. Experimental Section

2.1. Materials. The reactants used in this study were tetraethyl orthosilicate (TEOS) as a silica source, cetyltrimethylammonium bromide (CTAB) as a surfactant, $Ce(NO_3)_3 \cdot 6H_2O$ and $Fe(NO_3)_3 \cdot 9H_2O$ as Ce and Fe sources, respectively, and sodium hydroxide (NaOH), sodium fluoride (NaF), and deionized water. The typical composition for the synthesis of Ce-MCM-48 was: 1.0

* Corresponding author. E-mail: jlzhang@ecust.edu.cn. Telephone: +86-21-64252062. Fax: +86-21-64252062.

[†] Lab for Advanced Materials and Institute of Fine Chemicals, East China University of Science and Technology.

[‡] Graduate School of Engineering, Osaka Prefecture University.

10.1021/jp054024+ CCC: $30.25
Published on Web 10/13/2005

TEOS:0.65 CTAB:0.5 NaOH:62 H_2O:*x* $Ce(NO_3)_3$·6 H_2O:0.1 NaF, where $x = 0.005, 0.01, 0.02, 0.04$. The typical composition for the synthesis of Fe-MCM-48 was 1.0 TEOS:0.65 CTAB: 0.5 NaOH:62 H_2O:0.01 $Fe(NO_3)_3$·$9H_2O$:0.1 NaF.

2.2. Experimental Procedure. The Ce-MCM-48 and Fe-MCM-48 molecular sieves were prepared with fluoride addition as follows: 10 mL of tetraethyl orthosilicate (TEOS) was mixed with 50 mL of deionized water, and the mixture was vigorously stirred for 40 min at 35 °C, then 0.9 g of NaOH was added into mixture, and at the same time, 0.19 g of NaF was added into the mixture. After the NaF was added completely, the required content of $Ce(NO_3)_3$·$6H_2O$ or $Fe(NO_3)_3$·$9H_2O$ which are the Ce and Fe sources, respectively, were added. After another 60 min of vigorously stirring, 10.61 g of cetyltrimethylammonium bromide (CTAB) was added to the mixture, and stirring continued for 60 min. The mixture was heated for 24 h at 393 K in an autoclave under static conditions, and the resulting product was filtered, washed with distilled water, and dried at 373 K. The as-synthesized samples were then calcined in air for 4 h at 550 °C, increasing the temperature to 550 °C at 1 °C/min of the heating rate.

The mixture of SiO_2-CeO_2 (Si/Ce = 25) were also prepared by physical mixing for comparison purposes.

The procedure of synthesized Ce-MCM-48 and Fe-MCM-48 without fluoride addition was similar to the above procedure, but without NaF addition after NaOH was added into mixture.

The procedure of synthesized pure silica MCM-48 without fluoride addition was similar to the above procedure, but without NaF addition and without Ce and Fe source addition after NaOH was added into mixture.

2.3. Hydrothermal Stability Test. Calcined Si-MCM-48 (0.1 g), Ce-MCM-48 (0.1 g), or Fe-MCM-48 (0.1 g) was boiled for different periods of time in 100 mL of distilled water by using a flask equipped with reflux condenser. The X-ray powder diffraction (XRD) pattern was obtained after this boiled sample was subsequently filtered and dried in an oven at 413 K. According to the XRD analysis, loss in the XRD intensity, as compared with that of the same sample before the boiling water treatment, was used to judge the hydrothermal stability.

2.4. Characterization. X-ray powder diffraction (XRD) patterns of all samples were recorded on a Rigaku D/MAX-2550 diffractometer by using Cu Kα radiation of wavelength 1.541 Å, typically run at a voltage of 40 kV and current of 100 mA. N_2 adsorption and desorption isotherms were carried out by using Micromeritics ASAP 2010. For BET (Brunauer−Emmett−Teller method), the as-synthesized samples were calcined by following the procedures described in the Experimental Section, and the samples were then outgassed to remove moisture and impurities at 623 K for 5 h before measurement. The diffuse reflectance UV−visible (UV−vis) spectroscopy was recorded with a VARIAN Cary 500. The FTIR spectroscopy was obtained in the 400−4000 cm^{-1} range on a Nicolet Magna-IR550 (in Nujol using a KBr disk technique). The chemical analysis of Fe and Ce content in the calcined Fe-MCM-48 and Ce-MCM-48 samples was determined by atomic absorption by using a TJA IRIS 1000 instrument.

3. Results and Discussion

3.1. Chemical Analysis. Atomic absorption analysis of iron and cerium content in the samples prepared with fluoride addition was given. The corresponding Fe/Si and Ce/Si ratios in the starting gels were equivalent to 1.9 wt % and 20, 10, 5, 2.5 wt %, respectively. However, the Fe/Si and Ce/Si ratios in the solid samples were equivalent to 1.4 wt % and 18.1, 8.9, 3.9, 2.1 wt %, respectively. These values were lower than the corresponding Me/Si (Me = Fe, Ce) ratios in the starting gels, indicating that the Fe and Ce elements were only partially introduced into the MCM-48 matrix.

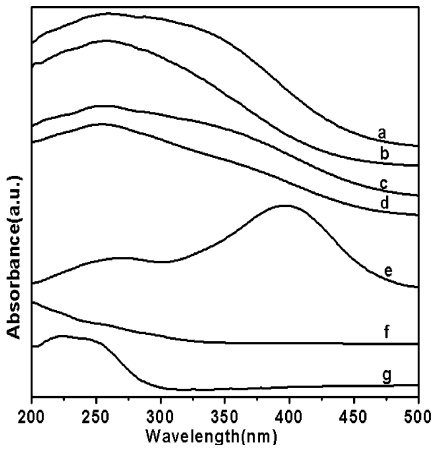

Figure 1. Diffuse reflectance UV−vis spectra of calcined Ce-MCM-48 with different Si/Ce ratios: (a) Si/Ce = 25, (b) Si/Ce = 50, (c) Si/Ce = 100, and (d) Si/Ce = 200; (e) SiO_2-CeO_2 with Si/Ce = 25, (f) calcined pure silica MCM-48, and (g) calcined Fe-MCM-48 with a Si/Fe ratio of 100.

3.2. Diffuse Reflectance UV−Visible Spectroscopy. The diffuse reflectance UV−vis spectroscopy is known to be a very sensitive probe for the identification and characterization of metal ion coordination and its existence in the framework and/or in the extraframework position of metal-containing zeolites.

Figure 1a−d depicts the UV−vis spectra of the calcined different Ce-containing Ce-MCM-48. The Ce-MCM-48 sample showed a broad absorption at 200−400 nm, and also, its intensity increased with an increase in the Ce content of the samples. However, the UV−vis spectrum of a silica and ceric oxide mixture (Si/Ce = 25) sample showed two distinct bands (see Figure 1e), a small absorption at ca. 300 nm, and a large absorption at ca. 400 nm. From Figure 1f, the UV−vis spectrum of pure silica MCM-48 sample showed no significant absorption at 200−500 nm. The position of ligand-to-metal charge-transfer ($O^2 \rightarrow Ce^{4+}$) spectra depends on the ligand field symmetry surrounding the Ce center. The electronic transitions from oxygen to cerium require higher energy for a tetracoordinated Ce^{4+} than for a hexacoordinated one.[28] Therefore, it may be inferred that the absorption band centered at ca. 300 nm for Ce-MCM-48 samples is due to the presence of one type of Ce^{4+} species (presumably in a tetracoordinated environment), whereas, in the case of a silica and ceric oxide mixture, two distinct bands, at 300 and 400 nm, correspond to two different types of Ce^{4+} species. The absorption at higher wavelength (∼400 nm) may be assigned to hexacoordinated Ce^{4+} species. The Ce-MCM-48 samples showed a broad absorption at 200−400 nm, which indicates that the Ce^{4+} ions in Ce-MCM-48 are present partly in tetrahedral coordination in the framework and partly as CeO_2 particles on the surface of framework. From Figure 1g, the Fe-MCM-48 sample showed a strong absorption in the 200−300 nm region (a clearly distinguished peak at $\lambda =$ 225 nm), attributed to the charge-transfer (CT) transitions involving isolated framework Fe^{3+} in $(FeO)_4^-$ tetrahedral geometry.[29]

3.3. FTIR Spectroscopy. The FTIR spectra in the framework and the hydroxyl region of purely siliceous and different Ce-containing MCM-48 samples showed bands characteristic of the mesoporous MCM-48-type materials, as shown in Figure

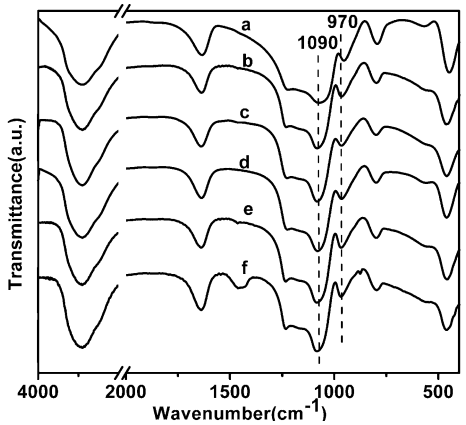

Figure 2. FTIR spectra of calcined (a) pure silica MCM-48, (b) Fe-MCM-48 with a Si/Fe of 100, and Ce-MCM-48 with different Si/Ce ratios: (c) Si/Ce = 200, (d) Si/Ce = 100, (e) Si/Ce = 50 and (f) Si/Ce = 25.

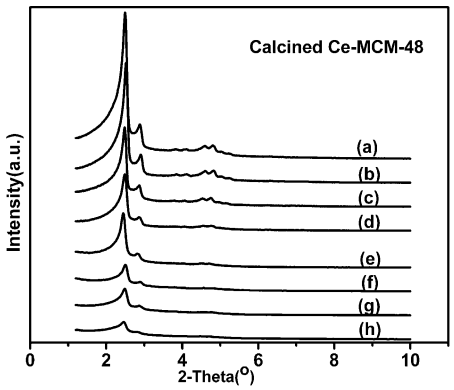

Figure 3. XRD patterns of calcined Ce-MCM-48 prepared in the presence of fluoride ions with different Si/Ce ratios: (a) Si/Ce = 200, (b) Si/Ce = 100, (c) Si/Ce = 50, and (d) Si/Ce = 25; prepared in the absence of fluoride ions with different Si/Ce ratios: (e) Si/Ce = 200, (f) Si/Ce = 100, (g) Si/Ce = 50, and (h) Si/Ce = 25.

2. In the framework region (400−1300 cm^{-1}), the vibration band at ca. 1090 cm^{-1} is assigned to ν_{as}(Si−O−Si). The band at ca. 970 cm^{-1}, observed for the Ce-MCM-48 and Fe-MCM-48 samples, can be assigned to a ν_{as}(Si−O−Ce) and ν_{as}(Si−O−Fe) vibration present in the framework of MCM-48. However, a band at ca. 965 cm^{-1} was also observed in the Si-MCM-48 sample. This band has been assigned to the Si−O stretching vibrations of Si−OH groups.[30] Therefore, this band cannot be taken as proof of Ce incorporation in the case of MCM-48 because a large number of silanol groups were always present in the calcined Si-MCM-48. However, it can be observed that the band lightly shifted to a higher wavenumber (970 cm^{-1}) in Ce-MCM-48 and Fe-MCM-48 samples compared with the wavenumber (965 cm^{-1}) in Si-MCM-48. It has also been observed that the ν_{as}(Si−O−Ce) band intensity lightly increased when Ce content increased (see Figure 2c−f). This is generally taken as proof of the incorporation of metal into the framework of microporous and mesoporous metallosilicates.[31] Therefore, it indicates that the Ce may be partly incorporated into the framework of MCM-48.

3.4. XRD Analysis. *3.4.1. Structural Ordering of Ce-MCM-48 and Fe-MCM-48.* Figure 3 shows the XRD patterns of calcined MCM-48 with different Si/Ce ratios synthesized with fluoride addition and without fluoride addition, respectively. According to Figure 3, the basal peaks (211) and (220), which can be indexed to *Ia*3*d* cubic structure, were all observed. The basal diffraction peak (211) shifted to higher 2θ values with the increase of Ce content. The d_{211} values are given in Table 1 along with the corresponding unit cell parameter (a_0) of different MCM-48 samples, calculated from the peak with *hkl* = 211 by using the equation $a_0 = d_{211}(6)^{1/2}$. A slight increase in the *d*-values and unit cell parameters was observed on incorporation of Ce. Although the increase in the *d*-values and unit cell parameters is not a monotic trend, the *d*-values and unit cell parameters of the Ce-MCM-48 are all larger than that of Si-MCM-48. The increase in unit cell parameter on Ce incorporation is probably due to the larger size of Ce^{4+} compared to that of Si^{4+}. Therefore, it may be inferred that Ce is partly incorporated into the framework position and/or walls of the silica network of MCM-48.[8]

TABLE 1: Results of d_{211} Spacing, and Unit Cell Parameter (a_0) of Me-MCM-48 (Me = Si and Ce) Samples

sample	F^-/Si mole ratio	$(Si/Ce)_{gel}$ mole ratio	d_{211}(Å)	a_0* (Å)
1	0	∞	33.7701	82.7195
2	0.1	200	34.5093	84.5302
3	0.1	100	34.1358	83.6153
4	0.1	50	34.6177	84.7957
5	0.1	25	34.6719	84.9285
6	0	200	35.1691	86.1463
7	0	100	35.2535	86.3531
8	0	50	34.5904	84.7288
9	0	25	35.0573	85.8725

*$a_{0=}$ $d_{211}(6)^{1/2}$.

In addition, from Figure 3, the XRD peaks of Ce-MCM-48 materials prepared with fluoride addition and without fluoride addition both became less resolved as the Ce content increased; meanwhile, the intensities of the (211) diffraction peak decreased with the increase in Ce content. It indicates that the structure orderings of the Ce-MCM-48 structure synthesized with fluoride addition and without fluoride both decreased with the increase in Ce content. This is probably due to an increasing number of defect sites and bond strain in these materials, as evidenced by the decreasing intensities of the (211) peak as well as the higher-angle peaks. However, it can be seen in Figure 3 that the XRD patterns of calcined Ce-MCM-48 samples with a Si/Ce ratio range between 200 and 50, prepared with fluoride addition, all clearly showed the eight diffraction peaks (211), (220), (321), (400), (420), (332), (422), and (431), which can be indexed to *Ia*3*d* cubic structure. However, in the XRD patterns of the samples with different Si/Ce ratios synthesized without fluoride addition, the secondary peaks were barely observed. It is known that the secondary peaks indicate long-range ordering of the MCM-48 structure.[32] It indicates that the long-range structure ordering of Ce-MCM-48 is significantly improved by adding fluoride ions with a F^-/Si ratio of 0.1. Additionally, the intensities of basal peaks (211) and (220) of Ce-MCM-48 with different Ce contents prepared in the presence of fluoride ions are much stronger than that prepared without fluoride addition. This indicates a higher organization of the pores when fluoride ions are present. According to the above results, the much more well-ordered structural Ce-MCM-48 can be obtained by adding fluoride ions with a F^-/Si ratio of 0.1, compared with the samples prepared without fluoride addition.

According to Figure 4, it can be seen that the basal peaks (211), (220), and the other secondary peaks can be clearly observed within the XRD patterns of as-synthesized and calcined Fe-MCM-48 prepared with fluoride addition. However, the XRD patterns of as-synthesized and calcined Fe-MCM-48 synthesized without fluoride addition only showed two basal peaks, (211) and (220), and the secondary peaks cannot be clearly observed. In addition, the intensity of the basal peaks of the samples

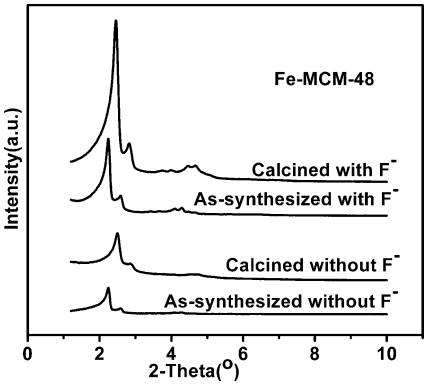

Figure 4. XRD patterns of as-synthesized and calcined Fe-MCM-48 with a Si/Fe of 100 prepared with fluoride addition and without fluoride addition, respectively.

prepared without fluoride addition is much lower than that of the samples prepared with fluoride addition. These results indicate that the long-range ordering of Fe-MCM-48 structure can be greatly enhanced by adding fluoride ions with a F^-/Si ratio of 0.1.

The addition of fluoride ions can improve the structure ordering of Ce-MCM-48 and Fe-MCM-48 mesoporous materials, which can be explained by the report of Voegtlin et al.[33] that the degree of polymerization of silicates can be enhanced in the presence of fluoride ions. F^- anions probably play a catalytic role favoring the polymerization of the silicate species. It causes a high charge density of the silicate network to improve the interactions between the cationic micelles and the anionic framework. Therefore, the pore ordering can be enhanced in the presence of fluoride ions. However, at the same time, the Ce and Fe incorporation can decline the structural ordering of mesoporous materials, and the structure ordering decreases with the increase of Ce content. Therefore, the structure ordering of Ce-MCM-48 and Fe-MCM-48 prepared with fluoride addition depends on the combined effect of fluoride ions added and content of incorporated heteroatoms.

3.4.2. Hydrothermal Stability of Ce-MCM-48 and Fe-MCM-48. According to Figure 5a, the mesoporous structure of Si-MCM-48 has completely collapsed after refluxing in boiling water for 12 h, which is in agreement with previous reports.[34−36] However, according to Figure 5b and c, the mesoporous structure is not completely lost; mesoporous structure is partly maintained after refluxing in boiling water for 12 h. When the Si/Ce ratio decreases to 25 (see Figure 5d), the mesoporous structure has completely collapsed after refluxing in boiling water for 12 h. It indicates that the low Ce content incorporated into the MCM-48 can enhance the hydrothermal stability of mesoporous materials (see Figure 5b and c). However, the high Ce content cannot efficiently enhance the hydrothermal stability (see Figure 5d). Similar observations were also reported by earlier workers, with Al incorporated into MCM-48.[26,27] Therefore, this result can explain that, when Ce is incorporated into the mesoporous materials, Si−O−Ce bonds, which are more resistant to attack from water compared to Si−O−Si bonds, are formed. In addition, the nonstructural Ce species on the surface can protect against water attack. However, the high Ce content can drastically degrade the structure ordering of Ce-MCM-48, leading to the decline of hydrothermal stability. Therefore, it is necessary to carefully control the Ce content to efficiently improve the hydrothermal stability of Ce-MCM-48. In this work, The Ce content in the Si/Ce ratio range between 100 and 50 improved the hydrothermal stability. It is also found that the degree of enhancement of hydrothermal stability by Ce incorporated into the mesoporous materials is not remarkable. Therefore, it is necessary to find another method to remarkably improve the hydrothermal stability of Ce-MCM-48.

Figure 6 shows the XRD patterns of calcined Ce-MCM-48 with different Si/Ce ratios synthesized with fluoride addition

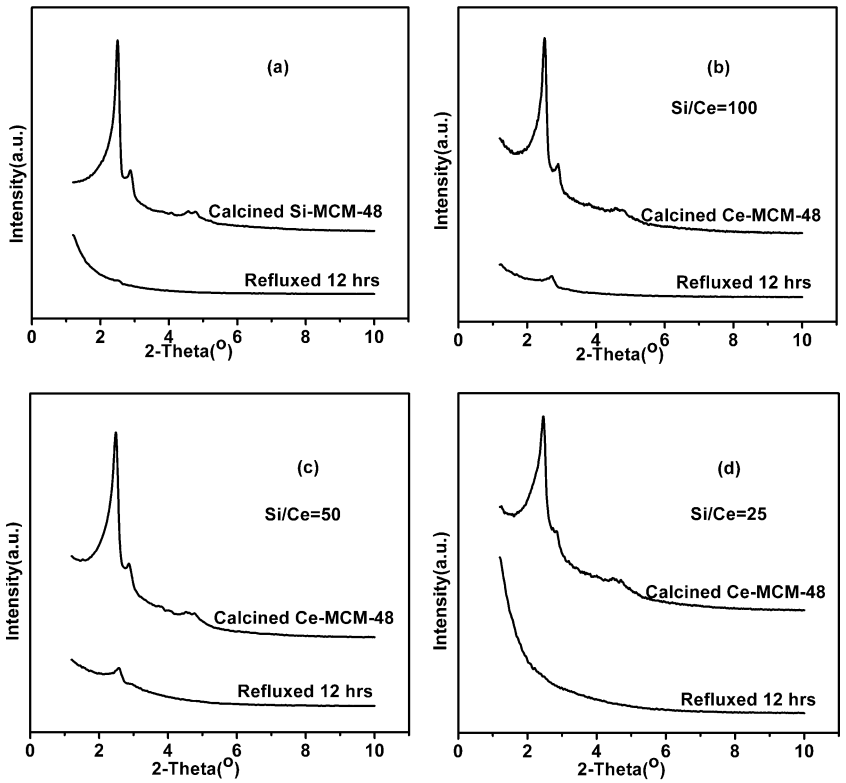

Figure 5. XRD patterns of calcined (a) Si-MCM-48 and Ce-MCM-48 with different Si/Ce ratios: (b) Si/Ce = 100, (c) Si/Ce = 50, and (d) Si/Ce = 25, all prepared without fluoride addition and treated in boiling water for different times.

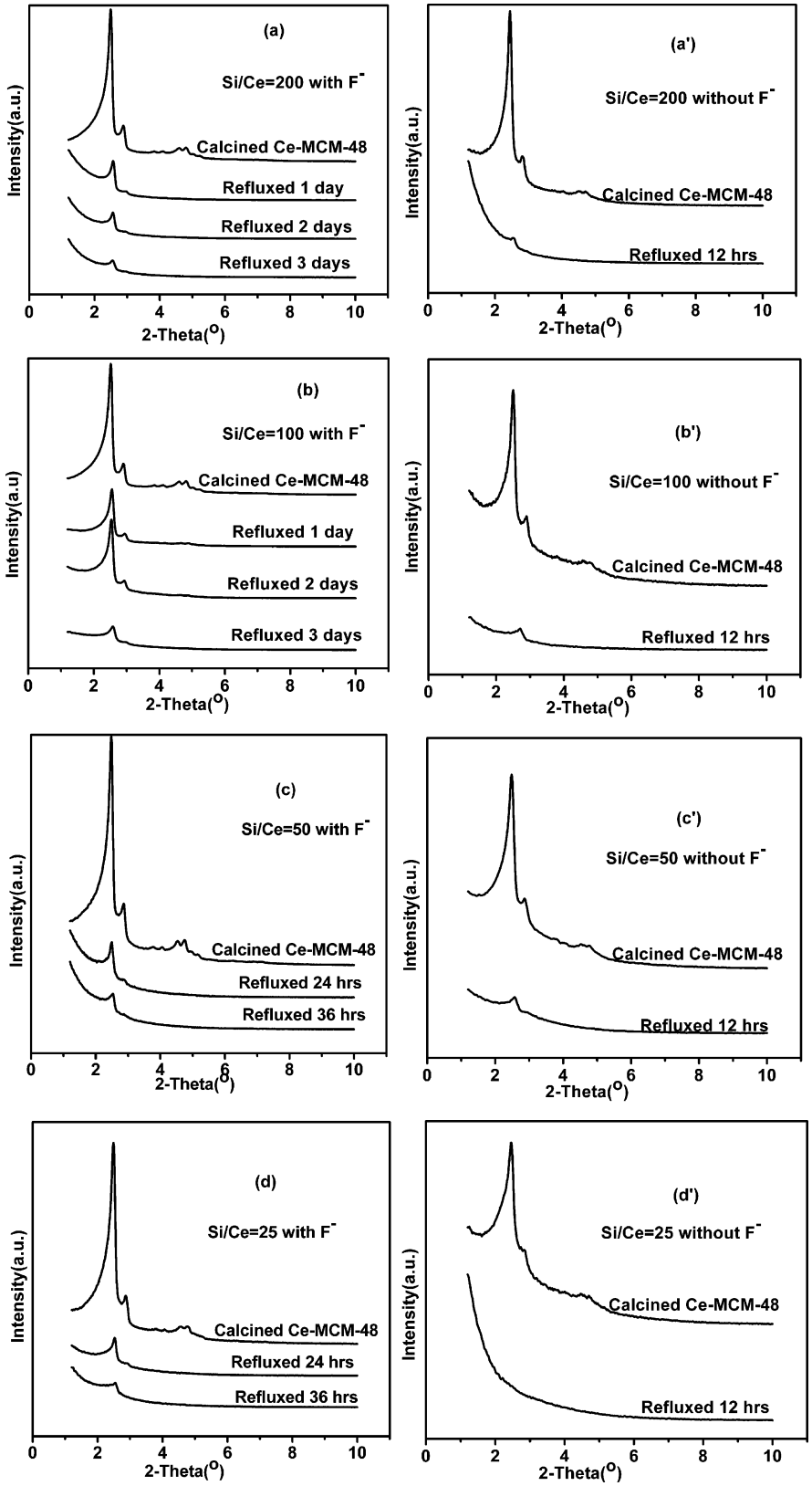

Figure 6. XRD patterns of calcined Ce-MCM-48 with different Si/Ce ratios, synthesized with fluoride addition and without fluoride addition, respectively, treated in boiling water for different times.

and without fluoride addition, respectively, which were treated in boiling water for different times. Figure 6a′ shows that the Ce-MCM-48 with a Si/Ce of 200 synthesized without fluoride addition almost completely loses its mesoporous structure after refluxing in boiling water for 12 h. However, when the samples were prepared by directly adding fluoride ions with F^-/Si ratio of 0.1 (see Figure 6a), the cubic ordering structure is still maintained even after refluxing in boiling water for 3 days, but the intensity of basal peak (211) gradually decreased with increasing the refluxing time in boiling water, which indicates that the ordering structure is gradually destroyed. For the samples prepared with fluoride addition, when the Si/Ce ratio

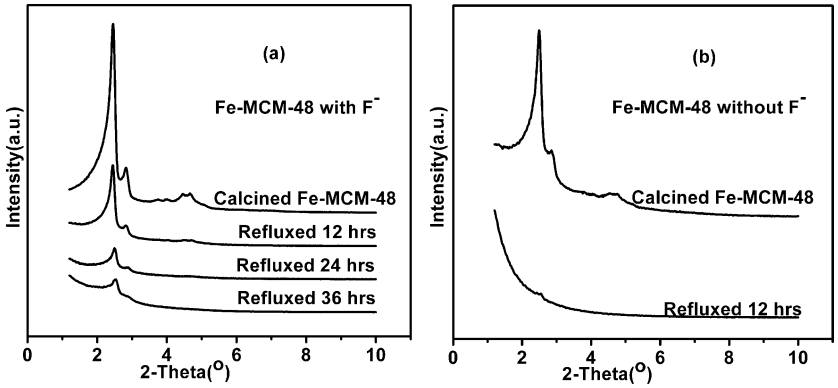

Figure 7. XRD patterns of calcined Fe-MCM-48 prepared (a) with fluoride addition, (b) without fluoride addition, with a Si/Fe of 100, refluxing in boiling water for different time.

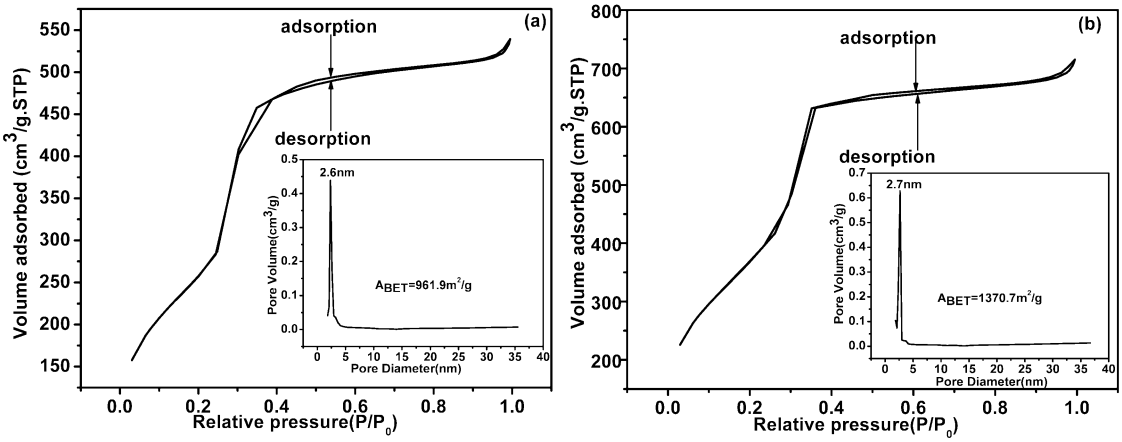

Figure 8. Adsorption−desorption isotherms of nitrogen at 77 K on calcined (a) Ce-MCM-48, (b) Fe-MCM-48 with a Si/Me of 100 (Me = Ce, Fe). The insert shows the BJH pore size distribution calculated from the desorption branch of the isotherm.

decreased from 200 to 100 (see Figure 6b), the cubic structure was also still maintained after refluxing in boiling water for 3 days. However, for the samples prepared without fluoride addition (see Figure 6b′), the mesoporous structure is almost destroyed after refluxing in boiling water for 12 h. When the Si/Ce ratio further decreases from 100 to 50, according to Figure 6c and c′, for the samples prepared without fluoride addition (see Figure 6c′), the mesoporous structure also almost collapsed after refluxing in boiling water for 12 h. However, for the samples synthesized with fluoride addition (see Figure 6c), the mesoporous structure at least can be maintained for 36 h in boiling water. However, the hydrothermal stability of the samples prepared by adding fluoride ions with a Si/Ce of 50 is much lower than that synthesized by adding fluoride ions with a Si/Ce of 200 and 100. When the Ce content decreases from 50 to 25, Figure 6d and d′ show the hydrothermal stability keeps on declining because of high Ce content resulting in the lower structure ordering of Ce-MCM-48, but the hydrothermal stability of the samples prepared with fluoride addition (see Figure 6d) is still much higher than that of the samples prepared without fluoride addition (see Figure 6d′). Additionally, for the samples prepared with fluoride addition, the stability in boiling water decreases in the following order: Ce-MCM-48-100 (Si/Ce = 100) > Ce-MCM-48-200 (Si/Ce = 200) > Ce-MCM-48-50 (Si/Ce = 50) > Ce-MCM-48-25 (Si/Ce = 25). This order implies that there is an optimum content of Ce with respect to the hydrothermal stability. This result can be explained by the result of Figure 5 that the appropriate Ce content incorporation can improve the hydrothermal stability of MCM-48 materials (see Figure 5). For the hydrothermal stability of Ce-MCM-48 samples prepared with fluoride addition, the hydrothermal stability depends on the effect of fluoride addition and incorporation of Ce. At the same content of fluoride addition, the hydrothermal stability of Ce-MCM-48 mainly depends on the Ce content. So the Ce-MCM-48 prepared in the presence of fluoride ions with a Si/Ce of 100 has the highest hydrothermal stability because of the appropriate Ce content incorporated. In summary, the hydrothermal stability of Ce-MCM-48 can be significantly improved by directly adding fluoride ions with a F^-/Si ratio of 0.1 to initial gel.

Figure 7 shows the XRD patterns of calcined Fe-MCM-48 with a Si/Fe of 100, synthesized with fluoride addition and without fluoride addition, respectively, with refluxing in boiling water for different times. According to Figure 7b, the sample synthesized without fluoride addition has a low hydrothermal stability, which completely loses its mesoporous structure after refluxing in boiling water for 12 h. It indicates that Fe incorporated into MCM-48 cannot improve the hydrothermal stability of MCM-48, which may be explained by the fact that the Fe−O−Si bonds and nonstructural Fe species on the surface have lower resistance to attack from water compared to that of Ce−O−Si bonds. However, for the sample prepared by directly adding NaF with a F^-/Si ratio of 0.1 (see Figure 7a), the cubic ordering structure is still maintained after refluxing in boiling water for 36 h. It indicates that the hydrothermal stability of Fe-MCM-48 can be enhanced by adding fluoride ions.

The above results can be explained by the fact that the F^- anions mainly directly affect the silicate to improve the degree of polymerization of silicate framework. Therefore, the hydrothermal stability of samples prepared with fluoride addition is significantly higher than that of the samples synthesized without fluoride addition. Meanwhile, the incorporation of Ce partly

improves hydrothermal stability of mesoporous materials; however, the incorporation of Fe cannot efficiently enhance hydrothermal stability of MCM-48. This result can be explained by the different effects of Ce−O−Si bonds and Fe−O−Si bonds and nonstructural Ce and Fe species on the surface to attack from water. However, the effect of fluoride addition is much more efficient on enhancement of hydrothermal stability than that of incorporation of Ce; the effect of the latter can be neglected compared to the former.

3.5. N_2 Adsorption and Desorption Analysis. Figure 8 presents the N_2 sorption isotherm of the Ce-MCM-48 and Fe-MCM-48 materials with a Si/Me of 100 (Me = Ce, Fe). In general, for mesoporous molecular sieves, the sharpness and height of the capillary condensation step in the isotherms indicate the pore size uniformity. From Figure 8, it can be found that both Ce-MCM-48 and Fe-MCM-48 materials exhibit typical type IV isotherms, with a typical capillary condensation step into uniform mesopores in the relative pressure (P/P_0) range 0.2−0.4. This indicates that both of the samples possess good mesopore structure ordering and a relatively narrow pore size distribution and that any structural changes resulting from the incorporation of Ce and Fe are not necessarily at the expense of pore uniformity. In addition, The Ce-MCM-48 material has a lower BET surface area of about 961.9 m^2/g compared to the Fe-MCM-48 material with a BET surface area of about 1370.7 m^2/g. However, they have similar pore sizes to the pore size of Ce-MCM-48 and Fe-MCM-48, which is 2.6 nm and 2.7 nm, respectively. However, they have different pore volumes, in that the former is 0.91 cm^3/g and the latter is 1.22 cm^3/g. Therefore, the different BET surface areas are the result of the different pore volumes. The pore wall thickness of Ce-MCM-48 and Fe-MCM-48, calculated from the pore diameter and the lattice parameter (a_0), according to the formula described by Ravikovitch et al.,[37,38] where wall thickness = $a_0/3.0919$ − pore size/2, where 3.0919 is a constant representing the minimal surface area for the MCM-48 *Ia*3*d* space group, which is 1.404 and 1.434 nm, respectively.

4. Conclusion

In summary, the hydrothermally stable and long-range ordered Ce-MCM-48 and Fe-MCM-48 were conveniently synthesized at 393 K for 24 h by directly adding fluoride ions to the initial gel without posttreatment and pH adjustment. The results of diffuse reflectance UV−vis spectroscopy and FTIR spectroscopy indicated that cubic phase Ce-MCM-48 and Fe-MCM-48 with tetracoordinated Ce^{4+}, Fe^{3+}, and nonstructural Ce and Fe on the surface were synthesized, respectively. The Ce-MCM-48 with a Si/Ce of 200 and 100, which was prepared by directly adding fluoride ions, could still maintain their mesoporous structures after refluxing in boiling water for 3 days. It was also found that Ce incorporated into the MCM-48 could partly enhance hydrothermal stability of MCM-48. The Fe incorporated into mesoporous materials could not enhance the hydrothermal stability of MCM-48. Additionally, the effect and reason for improvement of hydrothermal stability were different between the addition of fluoride ions and incorporation of Ce. The addition of fluoride ions mainly improved the degree of polymerization of silicate. However, the incorporation of Ce could form nonstructural Ce species on the surface and the Si−O−Ce bonds, which were more resistant to attack from water. The effect of fluorination was much more efficient on enhancement of hydrothermal stability than that of incorporation of Ce.

Acknowledgment. This work has been supported by National Basic Research Program of China (2004CB719500), the Shanghai Nanotechnology Promotion Center (0452nm010), and the Program for New Century Excellent Talents in University (NCET-04-0414).

References and Notes

(1) Kresge, C. T.; Leonowicz, M. E.; Roth, W. J.; Vartuli, J. C.; Beck, J. S. *Nature* **1992**, *359*, 710.

(2) Beck, J. S.; Vartulli, J. C.; Roth, W. J.; Leonowicz, M. E.; Kresge, C. T.; Schmitt, K. D.; Chu, C. T. W.; Olson, D. H.; Sheppard, E. W.; McCullen, S. B.; Higgings, J. B.; Schlenker, J. L. *J. Am. Chem. Soc.* **1992**, *114*, 10834.

(3) Ying, J. Y.; Mehnert, C. P.; Wong, M. S. *Angew. Chem., Int. Ed.* **1999**, *38*, 56.

(4) Corma, A. *Chem. Rev.* **1997**, *97*, 2373.

(5) Schumacher, K. *Microporous Mesoporous Mater.* **1999**, *27*, 201.

(6) Tanev, P. T.; Chibwe, M.; Pinnavaia, T. J. *Nature* **1994**, *368*, 321.

(7) Baltes, M.; Cassiers, K.; Van Der Voot, P.; Weckhuysen, B. M.; Schoonheydt, R. A.; Vansant, E. F. *J. Catal.* **2001**,*197*, 160.

(8) Laha, S. C.; Mukherjee, P.; Sainkar, S. R.; Kumar, R. *J. Catal.* **2002**, *207*, 213.

(9) Zhao, W.; Luo, Y. F.; Deng, P.; Li. Q. Z. *Catal. Lett.* **2001**, *73*, 199.

(10) Liu, Y.; Pinnavaia, T. J. *J. Mater. Chem.* **2002**, *12*, 3179.

(11) On, D. T.; Desplantier-Giscard, D.; Danumah, C.; Kaliaguine, S. *Appl. Catal., A:* **2002**, *222*, 299.

(12) Zhao, D.; Feng, J.; Huo, Q.; Melosh, N.; Fredrickson, G. H.; Chmelka, B. F.; Stucky, G. D. *Science* **1998**, *279*, 548.

(13) Coustel, N.; Renzo, F. D.; Fajula, F. *J. Chem. Soc., Chem. Commun.* **1999**, 967.

(14) Mokaya, R. *J. Phys. Chem. B* **1999**, *103*, 10204.

(15) Chen, L. Y.; Horiuchi, T.; Mori, T.; Maeda, K. *J. Phys. Chem. B* **1999**, *103*, 1216.

(16) Koyano, K. A.; Tatsumi, T.; Tanaka, Y.; Nakata, S. *J. Phys. Chem. B* **1997**, *101*, 9436.

(17) Zhao, X. S.; Lu, G. Q. *J. Phys. Chem. B* **1998**, *102*, 1556.

(18) Van Der Voort, P.; Baltes, M.; Vansant, E. F. *J. Phys. Chem. B* **1999**, *103*, 10102.

(19) Cassiers, K.; Linssen, T.; Mathieu, M.; Benjelloun, M.; Schrijnemakers, K.; Van Der Voort, P.; Cool, P.; Vansant, E. F. *Chem. Mater.* **2002**, *14*, 2317.

(20) Ryong, R.; Jun, S. *J. Phys. Chem. B* **1997**, *101*, 317.

(21) Kim, J. M.; Jun, S.; Ryong, R. *J. Phys. Chem. B* **1999**, *103*, 6200.

(22) Kruk, M.; Jaroniec, M.; Sayari, A. *Microporous Mesoporous Mater.* **1999**, *27*, 217.

(23) Brinker, C. J.; Scherer, G. W. *Sol−Gel Science*; Academic Press: London, 1990; pp 107 and 644.

(24) Xia, Q. H.; Hidajat, K.; Kawi, S. *Chem. Lett.* **2001**, 654.

(25) Kim, W. J.; Yoo, J. C.; Hayhurst, D. T. *Microporous Mesoporous Mater.* **2002**, *49*, 125.

(26) Xia, Y.; Mokaya, R. *J. Phys. Chem. B* **2003**,*107*, 6954.

(27) Xia, Y.; Mokaya, R. *Microporous Mesoporous Mater.* **2004**, *68*, 1.

(28) Kadgaonkara, M. D.; Lahaa, S. C.; Pandeyb, R. K.; Kumarb, P.; Mirajkara, S. P.; Kumar, R. *Catal. Today.* **2004**, *97*, 225.

(29) Inui, T.; Nagata, H.; Inoue, M. J. *J. Catal.* **1993**, *139*, 482.

(30) Decottiguies, M.; Phalippou, J.; Zarzycki, J. *J. Mater. Sci.* **1978**, *13*, 2605.

(31) Boccuti, M. R.; Rao, K. M.; Zecchina, A.; Leofanti, G.; Petrini, G. *Stud. Surf. Sci. Catal.* **1989**, *48*, 133.

(32) Kim, W. J.; Yoo, J. C.; Hayhurst, D. T. *Microporous Mesoporous Mater.* **2000**, *39*, 177.

(33) Voegtlin, A. C.; Ruch, F.; Guth, J. L.; Patarin, J.; Huve, L. *Microporous Mater.* **1997**, *9*, 95.

(34) Ryoo, R.; Kim, J. M.; Ko, C. H.; Shin, C. H. *J. Phys. Chem.* **1996**, *100*, 17718.

(35) Kawi, S.; Shen, S. C. *Mater. Lett.* **2000**, *42*, 108.

(36) Jun, S.; Kim, J. M.; Ryoo, R.; Ahn, Y. S.; Han, M. H. *Microporous Mesoporous Mater.* **2000**, *41*, 119.

(37) Ravikovitch, P. I.; Neimark, A. V. *Langmuir* **2000**, *16*, 2419.

(38) Schumacher, K.; Ravikovitch, P. I.; Du Chesne, A.; Neimark, A. V.; Unger, K. K. *Langmuir* **2000**, *16*, 4648.